Kinematics of Tau Lepton Decays

Aidan Bohenick

University of Colorado at Boulder

Department of Engineering Physics (EPEN)

Thesis Defense Committee:

Thesis Advisor: Prof. John Cumalat, Department of Physics
Honors Council Representative: Prof. Paul Beale, Department of Physics
Committee Member: Prof. Mark J. Ablowitz, Department of Applied Mathematics

Undergraduate Thesis
April 4$^{\text{th}}$, 2019

Abstract

In particle physics, when a particle decays, it is not always possible to fully reconstruct the decaying particle. This is due to the nature that some particles, such as neutrinos, do not typically interact and go straight through the detector unnoticed. This means when attempting to reconstruct the original mass of the decay, there will be missing information. Thus, the question is, even when there is missing information in a decay, is it possible to accurately reconstruct the decaying particle? In this project we will be focusing on the decay of $Z \rightarrow \tau_h \tau_h$, which will henceforth be referred to as a ditau decay, and the applicability of the reconstruction techniques discussed to other particles that undergo a ditau decay. This project focuses on the implementation of a new kinematic method for determining the momentum of a hadronically decaying 3-prong tau. Given this new way of determining the momentum, it has been tested on Monte Carlo samples before being run over data. What was found was that given this new technique, it is possible to reduce background contained in the reconstruction. This gives a higher signal significance for the ditau reconstruction. As signal significance is the figure of merit for discovery potential, this gives hope to the idea that the technique discussed will be able to be used on more than just Z decays.

Acknowledgements

I would like to express my very great appreciation to my research advisor, Dr. Cumalat, for giving me the opportunity to join the CMS group and to broaden my understanding of particle physics farther than I could have ever have hoped to achieve on my own. His valuable and constructive suggestions during the planning and development of this thesis was extremely helpful. His willingness to take me under his wing and give the time he could has been very much appreciated.

I would like to express my deep gratitude to Savanna Starko for her patient guidance, enthusiastic encouragement and useful critiques of this thesis. Her advice and assistance in keeping my progress on schedule was invaluable. The project would not be nearly at the level it currently is without her help.

Lastly, I would like to thank the BSM3G group, and more specifically, Brandon Soubasis and Alfredo Gurrola for their valuable support on this project. Whether the problem was conceptual or technical they were able to help me along and keep progress moving at a steady pace. Their kindness and help will not be forgotten.

Contents

1 Introduction

1.1 The Standard Model

The Standard Model (SM) of particle physics is a model that describes subatomic particles and their interactions. Through these interactions, we have four fundamental forces: the strong force, the weak force, electromagnetism, and gravity. All of the forces except for gravity are contained within the SM [10]. We are able to describe, individually, how each of these forces manifest in nature. The electromagnetic interaction is described using quantum electrodynamics (QED). When coupling QED with the weak interaction in order to describe a broader range of interactions we obtain electroweak theory (EW). Lastly, the strong interaction is described by quantum chromodynamics (QCD) [11]. We are able to combine these theories to form the symmetry group describing the SM:

$$SU(3)_C \times SU(2)_L \times U(1)_Y$$

where $SU(3)_C$ is the symmetry group describing QCD and $SU(2)_L \times U(1)_Y$ is the symmetry group describing electroweak theory [13]. We see that the electroweak theory is two parts as it is the unification of the electromagnetic and weak interactions.

The current SM is given in Figure 1. Subsets of particles contained within the SM experience these forces in different ways. The table is split into bosons and fermions, where bosons have integer spin and fermions have half-integer spin. Furthermore, the SM can be broken into three sub categories. These are represented by quarks, bosons, and leptons [14]. We note that the quarks and leptons come in three generations and that each subsequent generation is more massive than the previous [15] [16]. Also, all quarks and leptons have an associated anitparticle with identical mass and spin but opposite electrical charge (except for neutrinos which are electrically neutral). For every pair of quarks in a generation, the positively charged quark has electric charge $+2/3e$ and the negatively charged quark has electric charge -1/3e. This is different from the leptons, where each pair of leptons in a generation has one particle that is negatively charged with charge -e and a compliment neutrino which is electrically neutral.

Quarks are the fundamental particles that make up most matter that we see in the universe [17]. As the quarks are charged, this is what allows them to interact electromagnetically. We understand that quarks also interact via the strong force. They have a distinguishing factor referred to as color that dictates their strong force interactions. Quarks also

exhibit asymptotic freedom. This means that the attraction between quarks grows weaker as the quarks approach one another more closely and correspondingly that the attraction grows stronger as the quarks are separated [18]. Quarks combine together to form hadrons. Hadrons are divided into baryons and mesons. If we have a bound state of two quarks in the form of a quark-antiquark pair, this is called a meson. A bound state of three quarks is called a baryon [19]. The strong force is what keeps baryons and mesons held together. The up (u), charm (c), and top (t) form a family, and the down (d), strange (s), and bottom (b) form a family. The positively charged up quark and negatively charged down quark are the first generation. These quarks make up the majority of matter as they are the building blocks of protons, neutrons, and pions. The second generation is the positively charged charm quark and the negatively charged strange quark. The second generation forms hadrons such as kaons and lambdas. Lastly, the third generation is the positively charged top quark and the negatively charged bottom quark [20]. The third generation of quarks are very heavy and have very rapid decays. The bottom quark is sometimes found in exotic bound states, but the top quark, with a mean lifetime to be roughly 5×10^{-25}s, has such a rapid decay that it is never found in bound states as this lifetime is about a twentieth of the timescale for strong interactions [21]. We also note that normal matter is colorless. That is, a meson has one quark with a color and the other with that anti-color (i.e. the two quarks might be a red and an anti-red). In a bound state of three quarks, you have a red, green, and blue quark. This works out to be colorless as well [22].

Leptons interact electromagnetically and via the weak force predominantly. So, while the quarks interact via both the strong and electroweak forces, the leptons only experience the electroweak interaction [23]. For the leptons, the electron, muon, and tau form a family. Similarly, the electron neutrino, muon neutrino, and tau neutrino form a family [16]. The first generation consists of the electron (e) and the electron neutrino (ν_e). The electron is the most common lepton found in nature as it is responsible for electric current and forming shells around nuclei to create atoms. The second generation is the muon (μ) and the muon neutrino (ν_μ). Muons are heavier than electrons and with a mean lifetime of 2μs. When a muon decays it primarily decays to an electron, a muon neutrino, and an electron antineutrino [24]. Lastly, the third generation is the tau (τ) and the tau neutrino (ν_τ). The tau is the heaviest of the leptons with a mean lifetime of 0.3ps and can decay either leptonically or hadronically [1]. These decay will be discussed in greater detail later in the paper. Of the leptons, as discussed earlier, the electron, muon, and tau are charged with charge -e, while their corresponding neutrinos are electrically neutral.

In the SM we also have bosons, which are the force carriers of the SM. The interactions between between quarks and between leptons are mediated by the bosons. Currently, there are four gauge bosons in the SM; gluons (g), photons (γ), Z, and W [25]. All of the aforementioned bosons each have spin 1. Photons are the bosons that mediate the electromagnetic interactions. Gluons mediate the strong interactions. Finally, W and Z mediate the weak interaction. The W can have charge +1 (W^+) or -1 (W^-), while the photons, gluons, and Z are all electrically neutral. Currently, W and Z are the only massive bosons in the SM. The final boson, the scalar boson, is the Higgs boson. It is a spin 0 boson that comes as a consequence of the Higgs field [26].

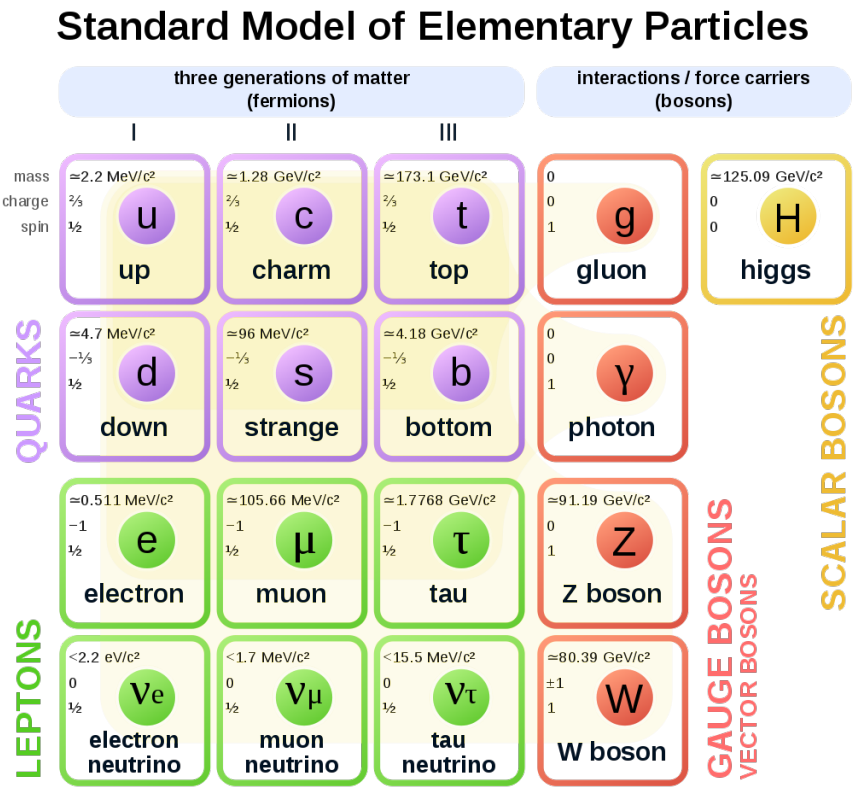

Figure 1: The current SM for particle physics.

1.2 The Z creation and decay

The different ways that the tau can decay and with what probabilities are given in the Appendix, Section 6.1, Table 6.1. We now define and differentiate what it means for a tau to decay leptonically versus hadronically. In either forms of the decay the tau first decays directly into a tau neutrino and a virtual W boson with a sign matching that of the tau. When a tau decays leptonically, the W boson will decay most often into either an electron and electron neutrino or muon and muon neutrino. Thus, due to the nature of neutrinos, the only visible products in the leptonic decay case are the electron or muon. The Feynman diagram for this decay is given by Figure 2.

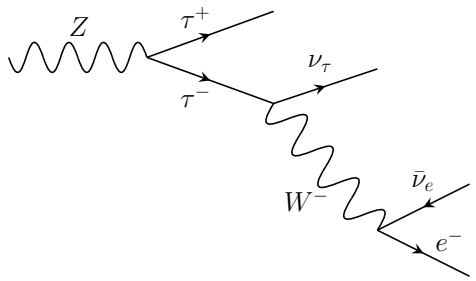

Figure 2: Leptonic τ decay

In the case that a tau decays hadronically, the W decays into a quark-antiquark pair. This pair will then rapidly hadronize into jets. These interact with gluons to create π^+, π^-, and pions (π^0s). Due to conservation of charge, there will always be an odd number of charged pions with net sign being the charge of the original tau. In the case that there is one charged pion present in the decay, we will refer to this as a 1-prong decay. In the case that there are three charged pions in the decay, we will refer to this as a 3-prong decay. The Feynman diagram for this decay is given by Figure 3. We can see that in this case there is only one neutrino, unlike the leptonic case where there are two neutrinos.

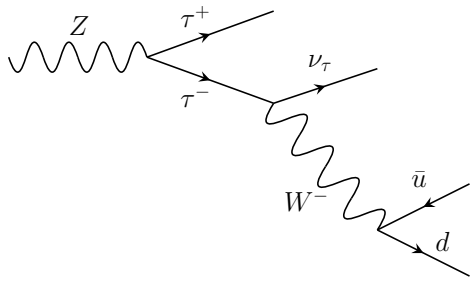

Figure 3: Hadronic τ decay

1.3 Beyond the Standard Model

We note that the SM is incomplete. The SM fails to answer many broad questions in particle physics. Some example questions that the SM fails to address are the identity of astronomical dark matter, the matter/antimatter asymmetry in the universe, and the hierarchy problem of why gravity is so much weaker when compared to the other forces governing particle interactions.

An example theory that is used in an attempt to help with this incompleteness is string theory. String theory is considered a promising candidate for describing gravitational systems at strong coupling and thus plays a prominent role in the description of black holes and evolution of the universe through the understanding of the origin of dark energy. Similarly, models with additional neutrino fields at the TeV scale provide a possible explanation for the mass of light neutrinos. New heavy particles are a common manifestation of these models, and we can potentially probe them at the Large Hadron Collider (LHC) [34].

As an aside, we discuss what symmetries are and the importance of them in particle physics. We know from Noether's Theorem that where there is a symmetry there is a conservation law. Some notable examples are time translation symmetry giving us energy conservation, space translation symmetry giving conservation of linear momentum, lorentz boost symmetry giving angular momentum conservation, and phases of wavefunction and gauged potential symmetries giving charge and current conservation. We note that gauge symmetries, in physics, is the observation that you can redefine the fields or particles in terms of each other, in such a way that the laws remain the same [27].

In order to attempt to resolve the incompleteness of the SM, we can introduce new gauge fields and interactions. A common manifestation of these gauge fields and interactions is heavy, neutral gauge bosons. This is because these heavy gauge bosons can be the gauge field of a new local broken symmetry. An example theorized heavy gauge boson that we will be focusing on is Z'. Z' is a hypothetical gauge boson that arises from extensions of the electroweak symmetry of the SM. There are several models of physics beyond the SM that predict Z' bosons with varying properties. Some examples include models with a new U(1) gauge symmetry [28], little Higgs models [29], and E_6 Grand Unified Theories (GUT) [30]. In models with a new $U(1)$ gauge symmetry, the Z' is the gauge boson of the broken symmetry. In little Higgs models, breaking of the global symmetry by gauge and Yukawa interactions generates Higgs mass and couplings at the TeV scale that cancel off the SM quadratic divergence of the Higgs mass from top, gauge, and Higgs loops. This results

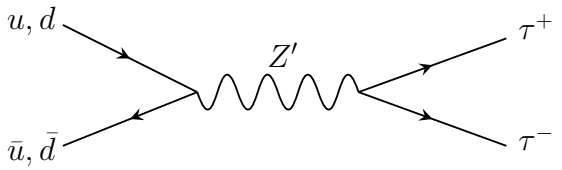

Figure 4: Feynman Diagram for a theoretical Z' decay.

in one of more Z' bosons. In Kaluza-Klein models, the Z' bosons arise as a result of hidden extra dimensions. We can see that the implications of these models gives hope of uncovering new physics at the TeV scale.

In searches for Z', models that include an extra Z'-like neutral gauge boson that decays to pairs of high p_T tau leptons are of particular importance. Although many models with extra gauge bosons obey the universality of the couplings (meaning the bosons decay to each generation of fermions with equal frequency), some models include generation-dependent couplings resulting in extra neutral gauge bosons that preferentially decay to tau leptons, making this analysis an important mode of discovery. The primary model studied in this project is the Sequential Standard Model Z'. This model assumes universality of the couplings (just like the SM Z) which makes it a useful benchmark both for testing other models and for tuning the search methodology [34].

In pp collisions at the LHC, the Z' is expected to be generated in much the same way as the SM Z. That is, Z' is to be primarily generated through Drell-Yan production via quark-antiquark interactions from the colliding protons. Since we are assuming Z' is a heavy neutral gauge boson with many of the properties of the more common Z-boson, a decay of interest for this analysis will be Z' to a pair of leptons, more specifically taus. This example creation and decay of Z' is given in Figure 4. In the choice to study decays to tau leptons, we place particular emphasis on current ditau mass reconstruction techniques. In this instance, we could apply current ditau reconstruction techniques in order to extrapolate back to a crucial property of the Z', its mass.

We aim to probe interactions involving Z' using particle physics technology like that available at the LHC.

Figure 5: A birds eye view of the LHC experiment.

1.4 LHC and CMS

The LHC is the world's largest and highest energy particle accelerator [2]. The LHC is a 27-km ring between 45 and 170 m underground that spans the border between France and Switzerland. The purpose of its creation is to accelerate proton beams to nearly the speed of light (about 3 m/s slower than c) prior to colliding them [3]. This is done by accelerating the protons in two counter rotating vacuum tubes being bent by 8.3 T superconducting dipole magnets [4]. The beams are crossed, thus creating collisions, at four locations along the length of the ring. These are the CMS, ATLAS, ALICE, and LHCb experiments. One of these experiments is the CMS experiment, which stands for Compact Muon Solenoid. With these collisions, we can probe particle interactions at very high energies.

When the beams collide, the relativistic energy of the collision can be transferred to the mass of new particles. At the CMS experiment, an incredible amount of this collision data is collected. The CMS experiment is 100 meters underground and is 21.6 meters long, 15 meters in diameter, and weighs about 14,000 tonnes, but we say it is compact in terms of the amount of data collected versus its size [5]. It is a cylindrical multilayered structure consisting of a "barrel" and two endcaps, with the LHC beam passing through the central axis of the cylinder. CMS focuses on the accurate detection of muons. For most outgoing particles of a collision, those particles experience the influence of the largest solenoid ever created. The magnetic field is created by a 4 Tesla magnetic field that is 100,000 times stronger than that of the Earth [8]. We will study collisions from the CMS experiment for this analysis.

The CMS detector is comprised of a silicon pixel and strip tracker, a lead tungstate

crystal electromagnetic calorimeter (ECAL), and a brass and scintillator hadron calorimeter (HCAL). Muons are measured in gas-ionization detectors embedded in the steel flux-return yoke outside the solenoid. We can see a slice of the CMS experiment in Figure 6 [6].

The silicon tracker is the innermost detector element in CMS and is designed to provide the highest resolution measurement of charged particle trajectories [7]. We refer to trajectories as "tracks." This tracker is composed of the pixel detector and the strip tracker. This system is able to obtain position data from the ionization of silicon as a charged particle passes through it. The next layer outward from the silicon tracker is the ECAL. The ECAL is made of crystals that are lead tungstate. We obtain information about charged particles in this section as charged particles deposit the majority of their energy here. Hence, the ECAL is designed primarily to measure the energies of photons and electrons. Surrounding the ECAL is the HCAL. The primary function of the HCAL is to measure the energies of hadrons. In order to accomplish this task the HCAL is made of brass from melted down artillery shells [9] interspersed with plastic scintillation panels. With this design, hadrons will deposit the remaining portion of their energy here. In most cases, electromagnetically-interacting particles are absorbed by the ECAL and don't make it to the HCAL. The solenoid is located just outside the HCAL system, but is contained inside the muon system. Lastly we have the muon chambers, which is the outermost layer of the detector. As its name would suggest, the primary function of the muon system is to detect any muons that occur within the interaction. The muon system is composed of drift tubes, cathode strip chambers, and resistive plate chambers.

For example, we can see from Figure 6 the electron has a curved path that stops within the ECAL. The reason that the electron's path bends is because, unlike the neutral hadron, it is charged. We see that it stops in the ECAL as this is where charged particles deposit most of their energy. We note that even though the photon is not charged this is also where it deposits its energy due to it interacting electromagnetically. Things like hadrons do not deposit the majority of their energy until they reach the HCAL. It should also be noted that the chief set of software tools used to reconstruct physics objects is a group of algorithms collectively referred to as Particle Flow (PF) [12].

We study current ditau mass reconstruction techniques in order to discern potential ways to improve upon their resolution. To date, only a lower bound for the mass of Z' candidates is confirmed at 2.5 TeV [31]. Thus, it is of high importance to find and develop new techniques in order to better reconstruct original masses of ditau decays. For the purposes

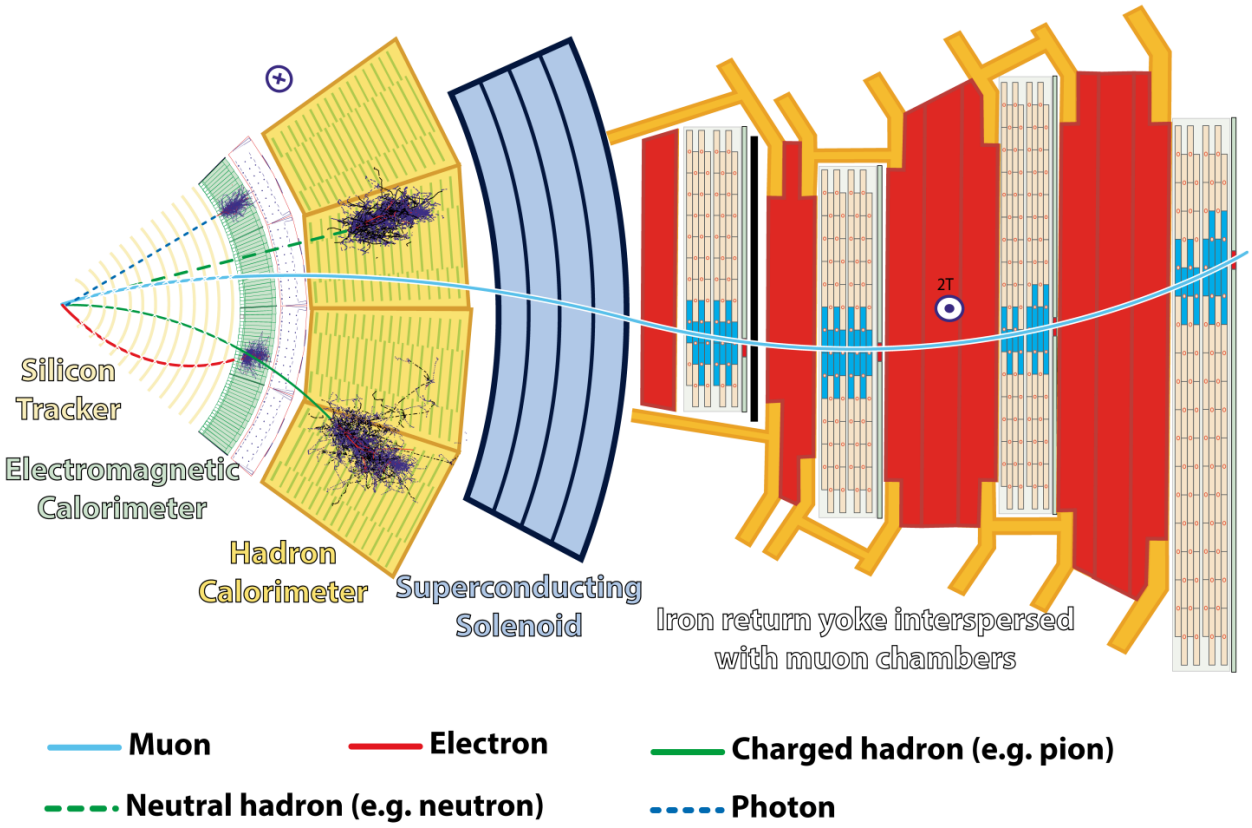

Figure 6: Slice of the CMS experiment

of this project, we will be testing any new reconstruction techniques on Z processes where Z decays to two tau leptons, as the mass of the Z is known to reasonable accuracy, allowing for a control region. Thus, if we are able to accurately reconstruct the mass of the Z, then this would give us confidence to apply the new ditau mass reconstruction technique in the context of Z' decays. These ditau mass reconstruction techniques have further utility since the reconstruction technique can be used on any particle that decays to ditau. Thus, this method could be used on the Higgs particle as the Higgs can decay via Z to ditau [32].

Two forms of data will be used for determining the accuracy of these methods. The first form of data will come from Monte Carlo (MC) simulation, and the other data being used will come from LHC, more specifically CMS.

1.5 Definition Area

We will now define some kinematic quantities that will be used throughout the rest of this paper. We note that the CMS experiment, which is where our data will come from, uses a right-handed coordinate system. In this system, the origin is set at the nominal pp collision point. For each of the axes, the x-axis points towards the center of the LHC ring, the y-axis points up, and the z-axis points along the beam line in the counter-clockwise direction. CMS also uses a pseudo-polar coordinate system. In this case we define ϕ as the azimuthal angle measured from the x-axis in the xy-plane. Next, θ is defined as the polar angle from the $+z$ axis. We also define η, the pseudorapidity, in terms of θ. The equation for this is given below.

Common terminology used in particle physics is the "transverse plane," which is the xy-plane perpendicular to the beam axis. Often times observable quantities are given in terms of their transverse component. We denote the transverse component of a term with a "T" subscript. As an example, particle momentum is often referred to in terms of its transverse component, p_T [33].

- p_T: Transverse momentum: $\sqrt{p_x^2 + p_y^2}$.
- E_T^{miss} (MET): Missing transverse energy: $E_T^{miss} = -\sum_{\text{detected particles}} \vec{p}_T$.
- m_T: Transverse mass which is obtained from transverse momentum and transverse energy: ($\Delta(\phi)$ is the difference in azimuthal angles between the tau p_T and the E_T^{miss}): $\sqrt{2 \times p_T(\tau_1) \times E_T^{miss} \times (1 - \cos(\Delta\phi))}$.
- η: Particle's angular position with respect to the beam direction: $\eta \equiv -\ln\left[\tan\left(\frac{\theta}{2}\right)\right]$.

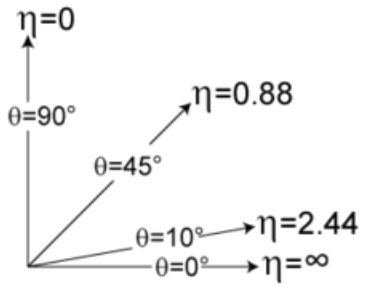

Figure 7: A visual representation of pseudorapidity (η)

2 Preliminary Analysis

2.1 Background and Signal Process

In order to understand the paradigm of data analysis in which we'll be applying the ditau mass reconstruction techniques, we must first understand what our signal process is and what background processes we will have to consider. The signal process is that which we are targeting. It contains the particle of interest, in this case Z', and we seek events of this type in our analysis. In the case of this project, we wish to understand particles that decay to ditau. SM backgrounds are other interactions and effects that are not the desired process, the signal process, but are being created in the interaction. This is because a SM background is a process that mimics the signal process. What we means by this is SM background processes have similar output products as the signal process. Thus, we must find ways to sift through or distinguish abundantly-produced and better known SM backgrounds from the desired signal process. Since a Z-boson can decay to a ditau pair, this type of event mimics the signal we seek. Hence, we must consider Z+jets processes as a SM background. There will be other SM backgrounds to consider as well. We note that in the remainder of this document, we focus on Z+jets events.

When protons collide, the relativistic energy of their collision can be transferred to mass energy of various kinds of particles. For example, we can also obtain W bosons, top quarks, and showers of jets. For reference, a jet is a highly energetic spray of particles. So, the question becomes how are we able to differentiate the two? That is, how do we tell the difference between signal process and background when both the signal process and the background can look the same? Some primary ways to differentiate signal and background is through the use of particle multiplicity or kinematic criteria. More terminology used in particle physics are the terms "cut" and "veto," which are interchangeable with selection criterion and rejection, respectively. Particle multiplicity takes advantage of the number and type of included particles in the topology. The kinematic criteria utilizes information about particle locations in the detector and how the particle should propagate.

Some examples of how we use particle multiplicity are vetoes of particular leptons or jet types and multiplicity requirements for leptons or jets. Two cuts of this type used in this analysis are the requirement of two taus in a decay and a "b-jet veto." The b-jet veto indicates that if a bottom quark is detected in the decay then the event will be discarded as it will not be part of the signal process. This is because b-jets will most often be coming from decays of top quark pairs, where each of t and $\bar{t}$ gives a W and a b-jet. Due to the

presence of W bosons in the stated decay, the process is able to mimic the signal process. Thus, this is a SM background that we can effectively reject with the b-jet veto.

Examples of kinematic criteria used are E_T^{miss} cut values, transverse momentum (p_T) thresholds for leptons or jets, or pseudorapidity (η) requirements for leptons or jets. A cut used in this analysis is the "discriminate by isolation."

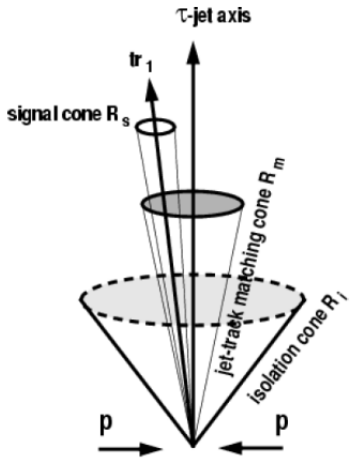

Figure 8: Visual representation of a cone used to determine isolation

The isolation of a particle is determined by drawing a fixed cone of size parameter $R = \sqrt{\eta^2 + \phi^2}$ around a particle candidate and summing the energies of all of the other particles (originating from the collision point) as measured in the tracker, ECAL, and HCAL. A visualization of this is given by Figure 8. The most commonly used definition of isolation is relative isolation, I_{rel}, which divides the sum of the energies deposited by the p_T of the candidate particle:

$$I_{rel} = \frac{\sum E_{tracker} + \sum E_{ECAL} + \sum E_{HCAL}}{p_T(candidate)}.$$

So, the isolation for a lepton describes the ratio of the other particles and products contained in some cone around the lepton track to the transverse momentum of that lepton. The other products include contributions to the energy from charged hadrons, neutral hadrons, photons, and pileup. Pileup is due to collisions happening every 250ns. As the detector has a delay before being able to obtain information about the current collision, the next collision is occurring theoretically before we obtain all of the information from the first in a series of two.

We make a requirement on how much of the other products can surround the lepton track with respect to the lepton transverse momentum. We make this cut so that we have a "cleaner" decay to observe and with which to work. An example of what the isolation cones would look like in a Z decay is given by Figure 9.

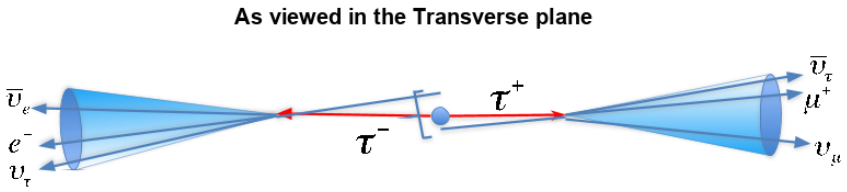

Figure 9: Example of Z' decaying to leptonically decaying taus and examples of what the isolation cone around the decay would look like.

As discussed before, a main background for $Z' \to \tau\tau$ is $Z \to \tau\tau$. Thus, it is of high importance to understand the Z decay, not just so that we have a control particle that we are able to test any new ditau reconstruction techniques on, but also because we must be sure we are able to differentiate it from the Z' decay. Thus, we introduce a control region (CR). The CR is the region used to test the Z+jets background estimation procedure. For the analysis performed in this project, the cuts used to define this CR are given in Table 2.1.

Name of cut	Requirement
Number of τs	2
MET (E_T^{miss}) cut	$>$ 30.0 GeV
bJet veto	on (medium WP)
τ: η cut	$<$ 2.1
τ: p_T cut	$>$ 60.0
τ: Disc by isolation	on (15%)
τ: Prong type	1 or 3 prongs (1or3hps)
diτ pair: Disc by OS	on
diτ pair: mass cut	70-110 GeV

Table 2.1: Cuts used for CR.

2.2 Standard Methods for ditau Mass Reconstruction

For a reconstruction technique of the mass to be considered optimal, we check that two conditions are satisfied. First, a good reconstruction technique will illustrate the mass of the Z-boson to be approximately 90 GeV [1]. This means that a plot of the ditau reconstructable mass will include a peak at 90 GeV. The narrower the peak, the better the resolution. Second, a good reconstruction technique will also reduce the contribution from SM backgrounds relative to signal contributions. This improves the signal significance, which we define as $S/\sqrt{S+B}$ in most instances where S is for signal events, and B is for background. We utilize the two conditions as a figure of merit to determine signal significance, which relates directly to discovery potential.

There are currently three standard methods being implemented for the reconstruction of ditau masses. These methods will be what we are comparing the results of a newly implemented technique (described later) to in order to determine if there is improvement in terms of the mass peak or if there is a decrease in the amount of background relative to signal. The three methods are referred to as the Standard method or Invariant Mass technique, the vector sum of visible products and E_T^{miss} (MET), and the Collinear approximation technique.

The Invariant Mass technique is the sum of the mass of the visible products of the ditau decay. We note that when we refer to mass we are referring to the 4-momentum of the visible products. In the case of a Z decay, we expect that this method will produce a mass peak below 90 GeV as the Invariant Mass technique does not take into account any information about the invisible products, such as neutrinos. The vector sum of visible products and E_T^{miss} reconstruction technique is similar to the invariant mass technique, where it is the sum of the mass of the visible products, but it has the added benefit of keeping track of the E_T^{miss} in the calculation of the mass. However, as E_T^{miss} does not accurately describe all of the vector information of the neutrino and is unable to discern between "real" E_T^{miss} and "fake" E_T^{miss} (discussed later), the vector sum of visible products and E_T^{miss} technique will be unable to exactly calculate the original mass of the decay. Last, we have the collinear approximation technique. This technique assumes that the E_T^{miss} is only coming from ν_τ and the mass of the tau is zero ($p \gg m$). It also assumes that the decay products are produced collinearly. The assumptions of this technique are accurate to high order, but the collinear approximation technique, like the vector sum of visible products and E_T^{miss} technique, will suffer from the same issues as discussed before.

Utilizing primarily Drell-Yan MC, we obtain the histograms given in Figure 10 where

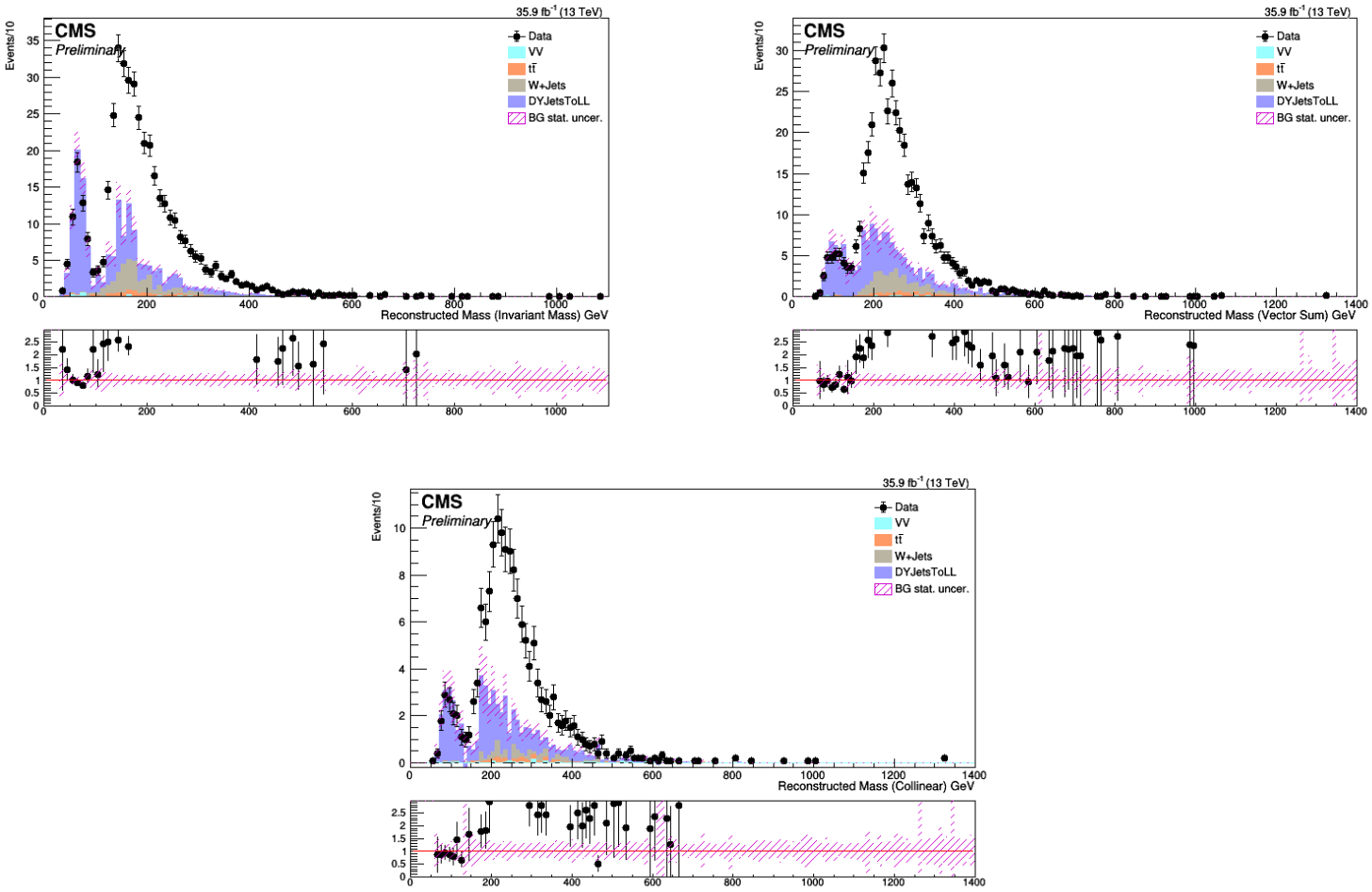

Figure 10: The three standard reconstruction techniques: (top left) Invariant Mass, (top right) Vector Sum of Visible Products and MET (E_T^{miss}), (bottom middle) Collinear Approximation

the top left histogram is the Invariant Mass technique, the top right histogram is the Vector Sum of Visible Products and MET (E_T^{miss}) technique, and the bottom middle histogram is the Collinear Approximation technique.

We can see that there is a large disagreement between the values obtained in the histogram and where the data lies. This is primarily due to QCD. The main contributing background at 150 GeV and higher is QCD multijet background. The diagram for this background is given in Figure 11.

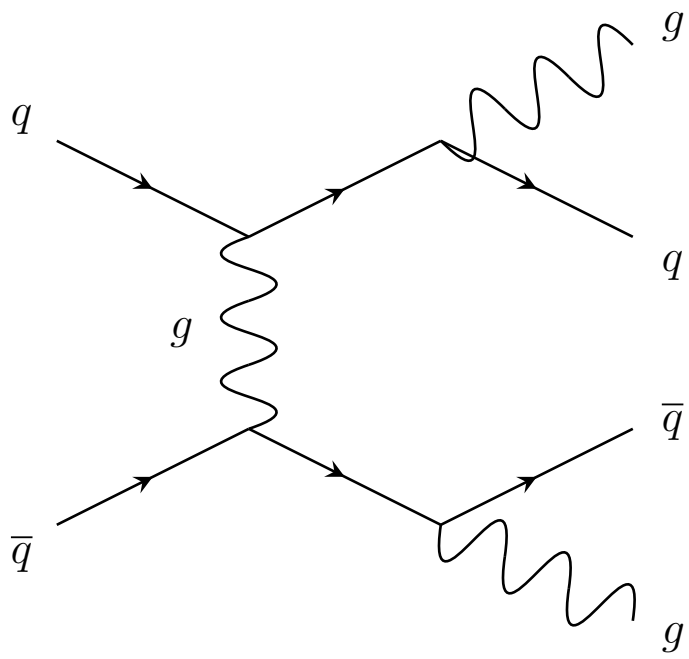

Figure 11: Feynman Diagram for QCD multijet background.

QCD is a primary contributing background because during the interaction two jets can be produced. When these jets are produced they are both able to "fake" a tau, where to "fake" means that a jet is misidentified as a lepton (tau in this case) due to its composition. This means that QCD can create a signal with a similar output to the signal process. However, unlike the b-jet veto as discussed earlier, it is more difficult and requires a more elegant solution in order to account for QCD, as well as to cut on it. Thus, for our results we do not take into account QCD as it is beyond the scope of our current analysis. This means that, in terms of the project, there is currently no need for an accurate representation of QCD.

2.3 Aside

As discussed earlier we now make an aside to discuss the difference between "real" E_T^{miss} and "fake" E_T^{miss}. This distinction is required due to the presence of both neutrinos and jets in the events being studied. We know that the colliding protons in the LHC have zero net transverse momentum. By conservation of momentum, it's expected the the particles generated from each pp collision will have net zero total transverse momentum. However, some particles, such as neutrinos, will evade CMS undetected. As mentioned before, this is due to the neutrinos being electrically neutral and only interacting weakly. This missing momentum we refer to as E_T^{miss}.

The "real" E_T^{miss} comes from particles which we cannot directly detect. An example, as we would expect, is any transverse momentum carried away by a neutrino. Any momentum carried by a neutrino will not be well measured by the detector. Hence, the p_T that it carries will be a contribution to the "real" E_T^{miss}. "Fake" E_T^{miss} often comes from mismeasurement. Even though the CMS detector has a high degree of accuracy, it is not perfect. For instance, if we measure the transverse momentum of a jet slightly off, that will add a contribution to the E_T^{miss}. However, as this is information that is not actually "missing," it will be a contribution to the "fake" E_T^{miss}. The combination of the "real" E_T^{miss} and the "fake" E_T^{miss} gives us the total E_T^{miss}, but we are unable to discern how much of the total is "real" or "fake."

2.4 Analysis of histograms

The peak of histograms given in Figure 10 represents where we expect the mass of the two taus to fall based on the kinematics. For example, if two tau particles comes from a Z-boson at rest, then we expect their masses to total near the mass of the Z-boson. In general for QCD multijet background, we have that the mass of the ditau created by this background is proportional to the transverse momenta of the two taus summed together. That is, $m(\tau_1, \tau_2) \propto p_T(\tau_1) + p_T(\tau_2)$. Since we have taus with a lower transverse momentum threshold of 60 GeV, the QCD multijet background contributes primarily in the tails (above 150 GeV) of the mass distribution. For Z+jets, if we assume that the system has no extra momentum (boost), it should be the case that each of the taus receive approximately 45 GeV from the Z-boson as the Z-boson has a rest mass of 90 GeV. Then, in the case of hadronically decaying taus, each of those taus are expected to decay to a hadronic tau (the visible products) and a tau neutrino. Thus, each hadronic tau should have approximately 23 GeV of the total momentum in a non-boosted scenario. Given our requirements on the lower threshold for tau transverse momentum at 60 GeV, this indicates that there could, for example, be some contribution to the momentum of the event from initial state radiation (ISR).

This is expected in the detector as ISR will most often come from instances where the incoming quarks in the collision radiate a gluon jet. The ISR-jet boosts the system, transferring some momentum by conservation laws to the Z-boson. This means that the Z-boson will have more energy to give to the subsequent taus created in the decay. We provide support for this idea by examining the transverse mass (m_T) plot for our control region. In analyses involving ISR, it has been found previously that it is often the case that the taus and neutrinos go in opposite direction of the ISR [35]. We know that the neutrinos will be the primary contribution to the E_T^{miss}. Thus, with the taus and neutrinos travelling nearly collinearly, the angle between the E_T^{miss} and the tau azimuthal direction will be small. Since the difference in azimuthal angles between the tau and the E_T^{miss} is small, we see from the dependence on $\Delta(\phi)$ in the m_T equation given in Section 1.5 that Z+jets, in this way, will contribute more at the low end of the m_T spectrum.

For QCD multijet, we get a larger contribution at the higher end of the m_T plot. If we imagine that those two jets are presumably back to back, the E_T^{miss} will likely come from mismeasurement of one of those two jets. Since the jets are nearly back-to-back, assume without loss of generality that the E_T^{miss} is aligned with the first jet. This means that the difference in azimuthal angles between the E_T^{miss} and the tau (from the second jet) is approaching π. Again, using the equation for m_T discussed in section 1.5, it is clear that $\Delta(\phi)$

would then be approaching π. As a result this would produce a higher value for m_T. This is the reason behind why QCD multijet contributes at the higher m_T end of the plot. But, how it the idea of ISR reflected in the transverse momentum plot?

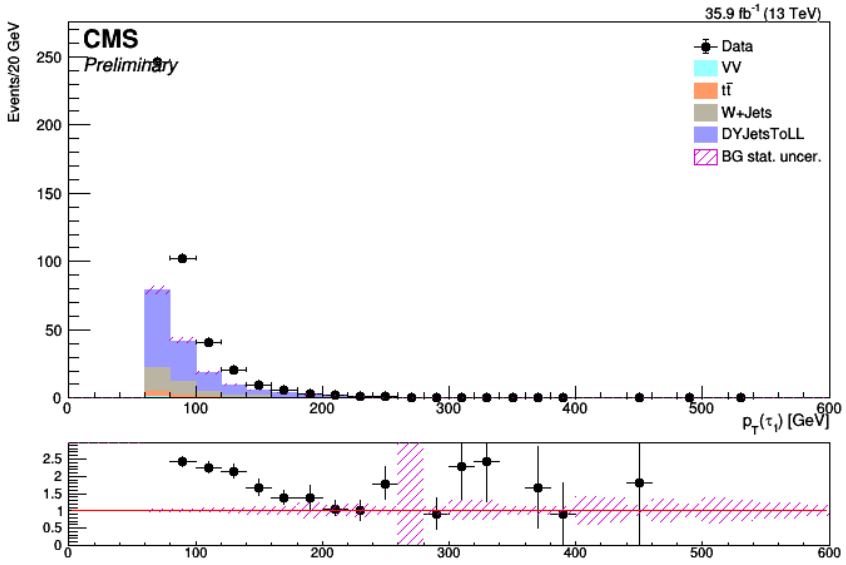

Figure 12: p_T of τ_1 generated from a Z decay.

From Figure 12 there is a better agreement between data and MC at the higher end of the transverse momentum plot. This reflects a good modeling of ISR, which provides a natural kinematic boost to the system.

If we operate knowing that the two jets from QCD multijet are nearly back-to-back, then the E_T^{miss} should lie along the direction of one of the two jets. For example, assume that both jets have 60 GeV momentum, but they are produced back-to-back. In this case there would be no E_T^{miss} as the net transverse momentum would be zero. However, if one of the two jets in the example was mismeasured by, for example, 10%, this would create a small fake E_T^{miss} contribution. For Z+jets the E_T^{miss} is going to be, on average, higher. Even in the non-boosted case, the two neutrinos are expected to have 45 GeV of momentum contributing to the E_T^{miss}. However, the E_T^{miss} will only increase with additional boost as the Z would then have more energy to give to the neutrinos in the decay. In order to see to what extent boost can affect our E_T^{miss} a example histogram of E_T^{miss} is given in Figure 13.

From the histogram it is clear that, on average, the E_T^{miss} created in a collision is usually low (below 100 GeV). However, considering our expected mass of Z is 90 GeV, it is possible

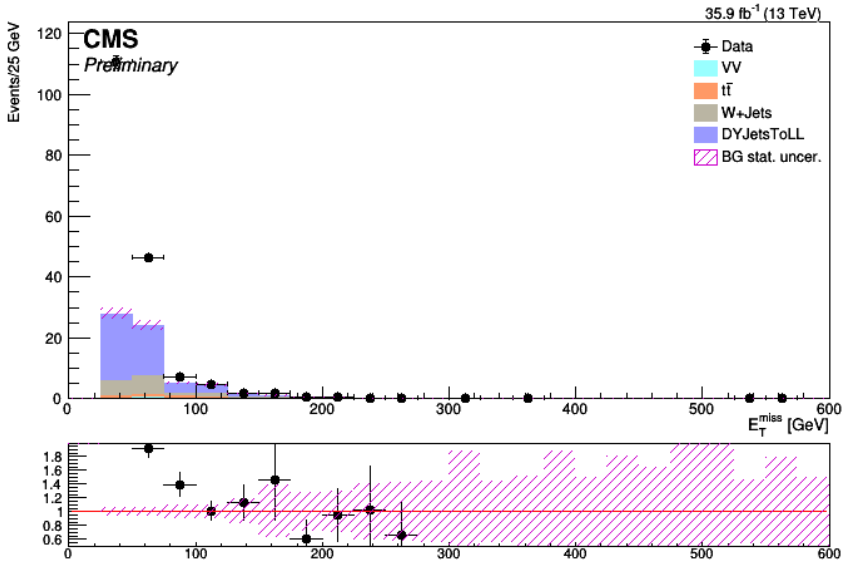

Figure 13: E_T^{miss} for Z decaying to a ditau lepton pair.

for the E_T^{miss} to have a very large effect when using one the standard ditau reconstruction techniques described in Section 2.2.

2.5 Test Cases and Analysis

In order to solidify the understanding we have about Z decays, we check several forms of kinematic criteria as they apply to these decays. First, using MC, we are able to find the percent of momentum that the neutrino carries away the original tau momentum. We are able to do this as, unlike in real data, a decay created by MC contains "all" information about said decay. This includes all information about any neutrinos that are present in the decay. Similarly, we are able to find the percent of the momentum carried away by the neutrino after the decay. The percent of the momentum carried by the neutrino and the percent of the momentum carried by the visible decay products are given in Figure 14 where the graph of the neutrino information is on the right and the graph of the visible products information is given on the left.

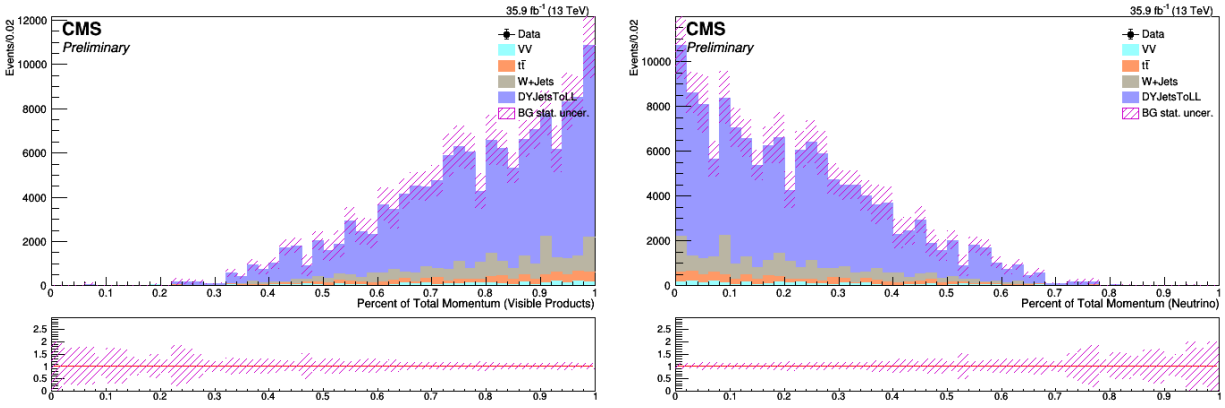

Figure 14: Fraction of the total momentum carried by the visible products (left) compared against the fraction of the total momentum carried by the neutrino (right).

From Figure 14 we can see that the trend of these plots is what we would expect. That is, the decay products will more often take the majority of the original total tau momentum. Thus, the neutrino, on average, will have a much smaller portion of the total tau momentum. On the assumption that our neutrino is produced at a pseudorapidity around zero, this supports our idea that our "real" E_T^{miss} will be low in comparison to the total transverse momentum of the system.

Next, we are able check the validity of our assumption that the neutrino is produced at a pseudorapidity around zero. Like before, plotting using MC information we find that the η of the neutrino from the original tau is given in Figure 15.

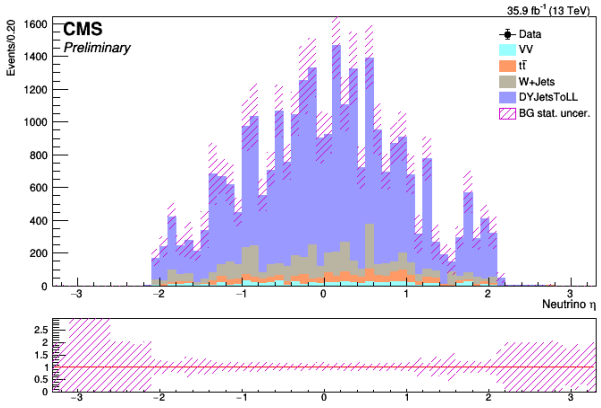

Figure 15: η of the neutrino with respect to mother τ.

Figure 15 shows that the neutrino is most often produced at an η of around zero,matching what is expected. This is expected because neutrinos are produced centrally (with pseudo-rapidity typically around zero).

Moving onto further kinematic criteria it is useful see a 2D histogram of the visible products fraction against the transverse momentum of the tau before the decay. This histogram is useful in that it would show if the fraction of the momentum taken by the visible products is dependent on the momentum of the original tau. This histogram is given in Figure 16.

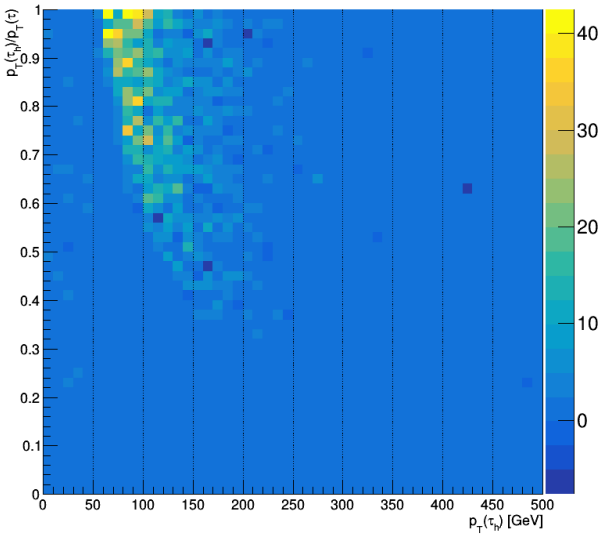

Figure 16: Fraction of the momentum carried by the visible products against the momentum of the original τ.

From this histogram in Figure 16 it is often the case that the fraction of the momentum carried away by the visible products is close to 1. As the momentum of the tau increases the trend is less predominant, but it remains true that the fraction of the momentum taken by the visible products is still the majority of the original momentum.

Similarly, it is possible to create a 2D histogram of the fraction momentum taken by the neutrino against the momentum of the tau before the decay. Before viewing the histogram, the expectation is there should be a similar trend as in Figure 14 where the histogram for the neutrino information is a mirror of the histogram for the visible product information. The 2D histogram for the fraction of the momentum taken by the neutrino is given in Figure 17.

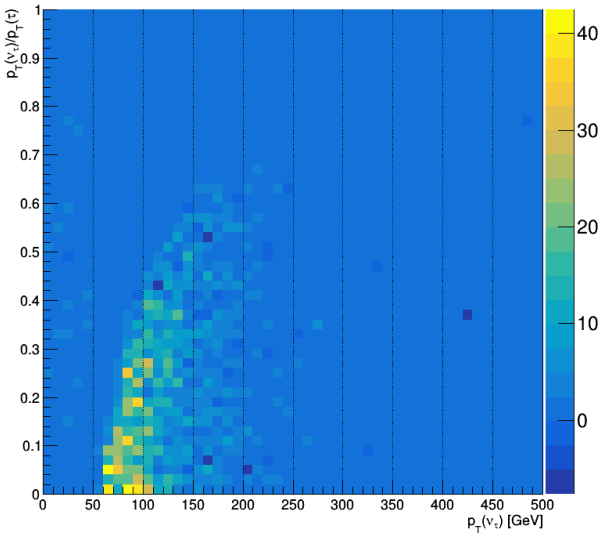

Figure 17: Fraction of the momentum carried by the neutrino against the momentum of the original τ.

As expected, the fraction of the momentum taken by the neutrino is inversely proportional to that of the fraction of the momentum taken by the visible products. That is, the fraction of the momentum taken by the neutrino is near zero, in contrast to the fraction of the momentum being taken by the visible products being near one. However, the trend mentioned before, where the data becomes more spread as the momentum of the tau increases remain true. This would indicate the potential for the neutrino to take a larger fraction of the momentum from the tau as the tau increases in momentum.

Since the hadronically decaying case is of particular interest to this project it would be wise to check what and if there is an effect on the momentum of the neutrino based on the type of hadronic decay. As defined in Section 1.2, when a tau decays hadronically it will either be a 1-prong decay or a 3-prong decay. So, when plotting the momentum of the neutrino against the mass of the hadronic visible products we obtain the histogram given in Figure 18. For clarity, the 1-prong decay case is given on the left and the 3-prong decay case is given on the right.

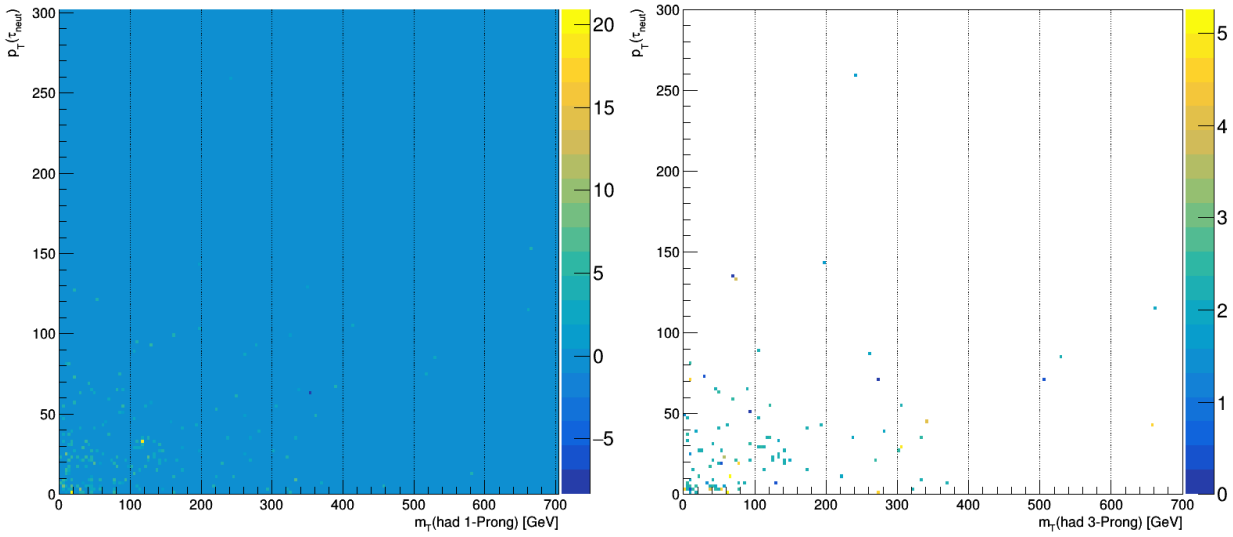

Figure 18: Mass of the visible products in a 1-prong decay against the momentum of the neutrino (left). Mass of the visible products in a 3-prong decay against the momentum of the neutrino (right).

What these histograms show is that in the 1-prong decay case the neutrino is much more likely to have a larger momentum. This is because in the 1-prong decay case the momentum of the neutrino is generally around 25 GeV where as in the case of the 3-prong decay the momentum is generally closer to zero. This makes sense because in the 3-prong case, when the original tau decays, there are more products that the tau must distribute its momentum to. What this means is that we expect a smaller effect from E_T^{miss} in the 3-prong case than the 1-prong case. In theory, this supports the idea that, when reconstructing the mass from a 3-prong decay, there will be better resolution in the reconstruction.

3 Development and New Analysis

3.1 New method implementation

For the development of a new methodology for reconstructing the ditau mass, the three prong hadronic decay of the tau particle will be used. This is because, in addition to the benefits already described in this paper: less neutrinos in the decay and a higher probability for the neutrino in the decay to have less of an impact on the reconstruction. With a 3-prong decay, it is possible to find the secondary vertex. This is done by finding the point where the tracks of the visible products intersect. We note that this is only possible with the 3-prong decay because the 3-prong decay will have three charged tracks that can be extrapolated back to a single point. In the 1-prong decay, as there is only one charged track, the secondary vertex cannot be found. Given that the location of the secondary vertex is now known, by balancing the transverse momentum it is now possible to find the primary vertex of the decay. In this section it will be shown that once this information is available and known, it can then be used to find the momentum of the original tau. This means that in the case of Z decaying to ditau, where both taus experience a 3-prong hadronic decay, it is possible to find the momentum of the tau from both sides. Once the momentum from both taus are known it is then possible to reconstruct the mass of the original ditau mass, which in the case of this project is Z. We note that it is actually only needed for one side of the ditau to decay to undergo a hadronic 3-prong decay, but for the analysis in the remainder of this paper we enforce the requirement that both taus in the ditau decay undergo a hadronic 3-prong decay.

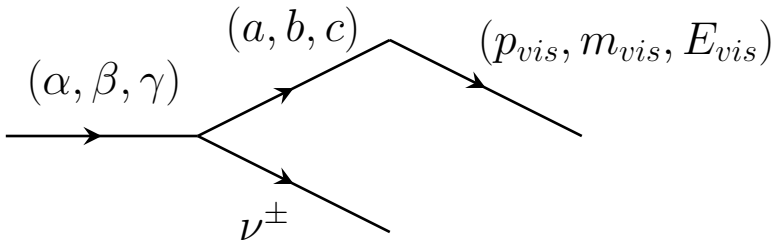

Figure 19: 3-Prong decay Vector Analysis

Figure 19 above will represent the 3-prong decay where, in vector coordinates, the tau direction is given by (α, β, γ), and the direction from the secondary vertex to where the visible products are created is (a, b, c). The visible products will have momentum, mass, and energy given by $(p_{vis}, m_{vis}, E_{vis})$, respectively. Similarly, the tau will have momentum, mass, and energy given by (p_τ, m_τ, E_τ), respectively. The full derivation for the kinematics that will be used in the remainder of this project is given in the Appendix, Section 6.2. Thus,

given the information specified earlier we define

$$M = \frac{m_\tau^2 + m_{vis}^2 - m_{inv}^2}{2E_{vis}}, \quad C = \frac{p_{vis}(\alpha a + \beta b + \gamma c)}{E_{vis}}$$

where E_{vis}, as stated before, is the energy of the visible products and p_{vis} is the momentum of the visible products. From this we can find the following equation for the momentum of the τ, p_τ:

$$|p_\tau| = \frac{MC \pm \sqrt{M^2C^2 - (1-C^2)(m_\tau^2 - M^2)}}{(1-C^2)}.$$

This allows for a new method for determining the momentum of the tau before the decay. Under the assumption that both taus undergo a 3-prong decay, it is then possible to perform the same calculations for the other tau produced in the decay of a ditau mass, namely Z. This means that now "all" information of the system is known. Thus, using the initial energy of the Z, the calculated momentum of each tau in the decay, and conservation laws, it is now possible to reconstruct the mass of the original Z to a high degree of accuracy.

3.2 Implementation of Code

The data analysis will be performed within the online infrastructure of the LHC Physics Center (LPC) at Fermilab (US). Specifically, the analysis framework is developed and maintained by the BSM3G working group of CMS. This is where the MC will be generated from and where all reconstruction techniques will be implemented. The MC samples used in this analysis are given in the Appendix, Section 6.4. To begin, when implementing this new kinematic technique, it must be enforced that only 3-prong decays are used. The kinematics derived in Section 3.1 will not work with any other decay as there will not be sufficient information. So, in order to verify that only 3-prong decays are used, the particle decay list will be used. The particle decay list is generator level information that tells the order in which particles are generated in a collision. The particle decay list also stores information such p_T values, η values, statuses of particles, particles IDs, and more. Particles are assigned an identification number according to the table in the Appendix, Section 6.3. For interactions used in this analysis the list will begin with two protons which collide and start the process.

It is possible to iterate through the particle decay list in order to find the indices of the tau particles. Under the assumption that the first taus encountered in the particle decay list are the taus created from a Z, the list need only be incremented until the index of the first two taus are found. This assumption is valid as it is know that there will be two taus in the decay due to the cuts implemented earlier, Table 2.1. It is also known that the first taus encountered in the decay list will have come from the Z by the generation order. It is possible to confirm this as the mother index of a particle is saved in the particle decay list. Thus, we are able to ensure that the mother of both the taus found is a Z. Next, in order to identify track number, the daughter particles of the taus (the particles to which the tau decays) will be counted.

The code used to find the tau particles and then to determine the number of charged tracks a given tau decay has is shown below. The first section of the code finds the index of the two taus in the particle decay list. Once the indices of the taus are know, it is then possible to iterate through the list again so see which of the particles have either of the taus as a mother particle. This is exactly what the next section of the code does. However, it must be remembered that as only 3-prong decays are desired, the tau must be the mother of three charged pions. Iterating through the particle decay list, if the tau does have a charged pion as a daughter particle, a counter representative of the number charged pion daughter is increment by one. This will help keep track of whether the decay is either a 1-prong decay or a 3-prong decay. In the case that the numbers of charged pion daughters is three, this

would correspond to a 3-prong decay.

```
int indexTau1 = 0;
int indexTau2 = 0;

for(size_t j = 0; j < _Gen->size(); j++){
  int id = abs(_Gen->pdg_id->at(j));
  int daughtCheck = _Gen->numDaught->at(j);
  if(id == 15 && indexTau1 == 0 && daughtCheck > 1){
    indexTau1 = j;
  }
  else if(id == 15 && indexTau2 == 0 && daughtCheck > 1){
    indexTau2 = j;
  }
}

int tau1Tracks = 0;
int tau2Tracks = 0;

for(size_t k = 0; k < _Gen->size(); k++){
  int id = _Gen->pdg_id->at(k);
  int mother = _Gen->BmotherIndex->at(k);
  if(abs(id) == 211 && mother == indexTau1){
    tau1Tracks++;
  }
  else if(abs(id) == 211 && mother == indexTau2){
    tau2Tracks++;
  }
}
```

Now that the 3-prong decays have been isolated, it is possible to implement the new method for finding the momentum of the taus. However, the vector information of the decay products is not stored in the analyzer explicitly in the form which we would prefer. This means that in order to test the new kinematics, a different way to perform an equivalent calculation is needed. Taking advantage of conservation laws, as show in the Appendix, Section 6.2, it is found that

$$p_\tau p_{vis}(\alpha a + \beta b + \gamma c) = P_x P'_x + P_y P'_y + P_z P'_z.$$

where these are variable are defined in Section 3.1. Since it is possible to define the energy and momentum of the visible products as

$$E_{vis} = E_\tau - E_\nu, \quad P_{vis} = P_\tau - P_\nu$$

it is now possible to use the information more readily available in the analyzer in order to test new kinematic method for finding the tau momentum, and consequently, reconstructing the ditau mass. The calculations are redefined using this information because the generator level tau information and the neutrino information is known and easily obtainable in MC. For reference, in order to use the code on real data the code will need to be rewritten to use vector information instead. However, the methodology is theoretically equivalent.

When reconstructing the original ditau mass the invariant mass technique will be used, but, now using the momentum of the tau obtained via the new kinematics. Note that, as a rule being used within the code, if when calculating the mass a negative value is obtained, it is instead set to zero. The negative values obtained in the calculations are due to the quadratic formula producing nonphysical solutions. As an example, if the discriminant is negative then this will produce a complex or imaginary solution. Thus, using the invariant mass technique with the newly found tau momentum on Z decaying to hadronically decaying taus, the histogram is given by Figure 20.

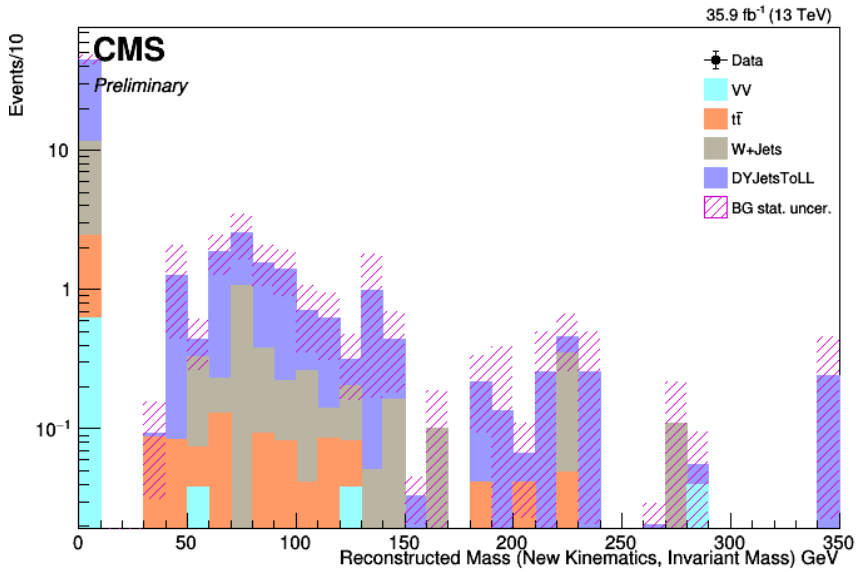

Figure 20: Log plot of a reconstructed ditau mass where both taus underwent a 3-prong decay.

3.3 Analysis of Results

We can see that we have a large amount of values put at zero, but the mass peak matched what we would expect from the invariant mass technique. In addition, we can also see that the background has been greatly reduced in the tails, which is promising for Z' studies since the signal presumably lies in the tails. Recall that signal significance, first discussed in Section 2.2, is defined as $S/\sqrt{S+B}$ where S is for signal events, and B is for background. In our analysis we have reduced the amount of background. This would imply that our signal significance is greater. As signal significance is the figure of merit for discovery potential this gives a promising outlook for the implementation of this method to detect new particles that decay to ditau, such as Z'.

4 Conclusion and Next Steps

This reconstruction technique developed in this paper is promising in terms of reconstruction of the Z-mass peak and the reduction of SM background events in the tail of the $m(\tau_h, \tau_h)$ distribution. However, this technique will need to undergo several rounds of validation and cross analyses. The method will also need to be modified to use vector information so that it may be implemented on real data. After the algorithm is able to handle real data, the next step will be to develop a technique so that the algorithm chooses the optimal solution. This is needed due to the nature of the quadratic formula producing two solutions. Part of future implementation and development of the algorithm will include using vertex information and global information in order to decide on which solution produced by the quadratic equation will be used for the reconstruction. We note that global information is using information from both of the taus together, rather than treating each tau individually. This could include choosing the solutions from each tau so that decays are back-to-back. Finally, after the modifications have been made and the method has been verified in it's ability to accurately reconstruct Z, a next step will be implementing and testing the technique with Z' signal samples.

5 Bibliography

References

[1] M. Tanabashi et al. (Particle Data Group) (2018). "Review of Particle Physics". *Physical Review D.* 98 (3): 030001. doi:10.1103/PhysRevD.98.030001.

[2] CERN-Brochure-2017-002-Eng.pdf. (n.d.). Retrieved from `https://pt.scribd.com/document/360544784/CERN-Brochure-2017-002-Eng-pdf`.

[3] Deboy, D.; Assmann, R.W.; Burkart, F.; Cauchi, M.; Wollmann, D. (29 August 2011). "Acoustic measurements at LHC collimators" (PDF). *LHC Collimation Project.*

[4] Stephen Myers (4 October 2013). "The Large Hadron Collider 2008-2013." *International Journal of Modern Physics A.* 28 (25): 1330035–1–1330035–65. Bibcode:2013IJMPA..2830035M. doi:10.1142/S0217751X13300354.

[5] "Why is CMS so big?" `http://cms.web.cern.ch/news/why-cms-so-big`.

[6] "Detector overview - CMS Experiment." `http://cms.web.cern.ch/news/detector-overview`.

[7] "Tracker detector - CMS Experiment." `http://cms.web.cern.ch/news/tracker-detector`.

[8] "Superconducting Magnet - CMS Experiment." `http://cms.web.cern.ch/news/superconducting-magnet`.

[9] "Using Russian navy shells - CMS Experiment." `http://cms.web.cern.ch/news/using-russian-navy-shells`

[10] The Standard Model. (n.d.). Retrieved from `http://home.web.cern.ch/about/physics/standard-model`

[11] "Standard Model of Particles and Interactions." *jhu.edu.* Johns Hopkins University. Archived from the original on March 4, 2016.

[12] F. Beaudette [CMS Collaboration], "The CMS Particle Flow Algorithm," arXiv:1401.8155 [hep-ex].

[13] According to experiments the gauge group is $SU(3) \times SU(2) \times U(1)/Z$ where Z is a subset of Z_6: Tong, David (2017). "Line operators in the Standard Model." *Journal of High Energy Physics*. 2017 (7). doi:10.1007/jhep07(2017)104. ISSN 1029-8479

[14] Mark Thomson (5 September 2013). *Modern Particle Physics*. Cambridge University Press. ISBN 978-1-107-29254-3.

[15] C. Quigg (2006). "Particles and the Standard Model." In G. Fraser. *The New Physics for the Twenty-First Century*. Cambridge University Press. p. 91. ISBN 978-0-521-81600-7.

[16] R. Nave. "Leptons." *HyperPhysics*. Georgia State University, Department of Physics and Astronomy.

[17] "Quark (subatomic particle)." *Encyclopædia Britannica*.

[18] F. Wilczek; B. Devine (2006). *Fantastic Realities*. World Scientific. pp. 400ff. ISBN 978-981-256-649-2.

[19] Section 6.1. in P. C. W. Davies (1979). *The Forces of Nature*. Cambridge University Press. ISBN 978-0-521-22523-6.

[20] K. A. Olive; et al. (Particle Data Group) (2014). "Review of Particle Physics." *Chinese Physics C*. 38 (9): 090001. Bibcode:2014ChPhC..38i0001O. doi:10.1088/1674-1137/38/9/090001

[21] A. Quadt (2006). "Top quark physics at hadron colliders". *European Physical Journal C*. 48 (3): 835–1000. Bibcode:2006EPJC...48..835Q. doi:10.1140/epjc/s2006-02631-6

[22] B. A. Schumm (2004). *Deep Down Things*. Johns Hopkins University Press. pp. 131–132. ISBN 978-0-8018-7971-5.

[23] "Lepton (physics)." *Encyclopedia Britannica*.

[24] J. Beringer et al. (Particle Data Group) (2012). "PDGLive Particle Summary 'Leptons (e, mu, tau, ... neutrinos ...)'" (PDF). Particle Data Group.

[25] Veltman, Martinus (2003). *Facts and Mysteries in Elementary Particle Physics*. World Scientific. ISBN 981-238-149-X.

[26] Onyisi, P. (23 October 2012). "Higgs boson FAQ." University of Texas ATLAS group.

[27] Neuenschwander, Dwight E. (2010). *Emmy Noether's Wonderful Theorem*. Johns Hopkins University Press. ISBN 978-0-8018-9694-1.

[28] G. Altarelli, B. Mele, and M. Ruiz-Altaba. Searching for new heavy vector bosons in $p\bar{p}$ colliders. *Zeitschrift fur Physik C Particles and Fields*, 45(1):109-121, 1989.

[29] Andrea Lami and Pablo Roig. $H \to \ell\ell'$ in the simplest little Higgs model. *Phys.Rev.*, D94(5):056001, 2016.

[30] David London and Jonathan L. Rosner. Extra gauge bosons in E_6. *Phys. Rev. D*, 34:1530-1546, Sep 1986.

[31] Okada, Nobuchika, and Satomi Okada. "Z'_{BL}Portal Dark Matter and LHC Run-2 Results." *Physical Review D*, vol. 93, no. 7, 2016, doi:10.1103/physrevd.93.075003.

[32] "Higgs bosons: theory and searches" (PDF). *PDGLive*. Particle Data Group. 12 July 2012.

[33] Wong, C. (1994). `Introduction to high-energy heavy-ion collisions`. Singapore: World Scientific.

[34] Gurrola, A., 2017, *Context for Z' in Particle Physics*, lecture notes, Vanderbilt University, 2 April 2019.

[35] Flórez, A., Bravo, L., Gurrola, A., Ávila, C., Segura, M., Sheldon, P., & Johns, W. (2016). Probing the stau-neutralino coannihilation region at the LHC with a soft tau lepton and a jet from initial state radiation. *Physical Review D*, 94(7). doi:10.1103/physrevd.94.073007

6 Appendix

6.1 Table of τ Branching Fractions

decay mode	fit result (%)	coefficient
$\mu^-\bar{\nu}_\mu\nu_\tau$	17.3936 ± 0.0384	1.0000
$e^-\bar{\nu}_e\nu_\tau$	17.8174 ± 0.0399	1.0000
$\pi^-\nu_\tau$	10.8165 ± 0.0512	1.0000
$K^-\nu_\tau$	0.6964 ± 0.0096	1.0000
$\pi^-\pi^0\nu_\tau$	25.4940 ± 0.0893	1.0000
$K^-\pi^0\nu_\tau$	0.4329 ± 0.0148	1.0000
$\pi^-2\pi^0\nu^\tau$ (ex. K^0)	9.2595 ± 0.0964	1.0021
$K^-2\pi^0\nu_\tau$ (ex. K^0)	0.0648 ± 0.0218	1.0000
$\pi^-3\pi^0\nu_\tau$ (ex. K^0)	1.0428 ± 0.0707	1.0000
$K^-3\pi^0\nu_\tau$ (ex. K^0, η)	0.0478 ± 0.0212	1.0000
$h^-4\pi^0\nu_\tau$ (ex. K^0, η)	0.1119 ± 0.0391	1.0000
$\pi^-\bar{K}^0\pi^0\nu_\tau$	0.8395 ± 0.0140	1.0000
$K^-K^0\nu_\tau$	0.1479 ± 0.0053	1.0000
$\pi^-\bar{K}^0\pi^0\nu_\tau$	0.3821 ± 0.0129	1.0000
$K^-\pi^0K^0\nu_\tau$	0.1503 ± 0.0071	1.0000
$\pi^-\bar{K}^0\pi^0\pi^0\nu_\tau$ (ex. K^0)	0.0263 ± 0.0226	1.0000
$\pi^-K^0_SK^0_S\nu_\tau$	0.0233 ± 0.0007	2.0000
$\pi^-K^0_SK^0_L\nu_\tau$	0.1080 ± 0.0241	1.0000
$\pi^-\pi^0K^0_SK^0_S\nu_\tau$	0.0018 ± 0.0002	2.0000
$\pi^-\pi^0K^0_SK^0_L\nu_\tau$	0.0325 ± 0.0119	1.0000
$\bar{K}^0h^-h^-h^+\nu_\tau$	0.0247 ± 0.0199	1.0000
$\pi^-\pi^-\pi^+\nu_\tau$ (ex. K^0, ω)	8.9870 ± 0.0514	1.0021
$\pi^-\pi^-\pi^+\pi^0\nu_\tau$ (ex. K^0, ω)	2.7404 ± 0.0710	1.0000
$h^-h^-h^+2\pi^0\nu_\tau$ (ex. K^0, ω, η)	0.0980 ± 0.0356	1.0000
$\pi^-K^-K^+\nu_\tau$	0.1435 ± 0.0027	1.0000
$\pi^-K^-K^+\pi^0\nu_\tau$	0.0061 ± 0.0018	1.0000
$\pi^-\pi^0\eta\nu_\tau$	0.1389 ± 0.0072	1.0000
$K^-\eta\nu_\tau$	0.0155 ± 0.0008	1.0000
$K^-\pi^0\eta\nu_\tau$	0.0048 ± 0.0012	1.0000
$\pi^-\bar{K}^0\eta\nu_\tau$	0.0094 ± 0.0015	1.0000

$\pi^-\pi^+\pi^-\eta\nu_\tau$ (ex. K^0)	0.0219 ± 0.0013	1.0000
$K^-\omega\nu_\tau$	0.0410 ± 0.0092	1.0000
$h^-\pi^0\omega\nu_\tau$	0.4085 ± 0.0419	1.0000
$K^-\phi\nu_\tau$	0.0044 ± 0.0016	0.8310
$\pi^-\omega\nu_\tau$	1.9494 ± 0.0645	1.0000
$K^-\pi^-\pi^+\nu_\tau$ (ex. K^0, ω)	0.2927 ± 0.0068	1.0000
$K^-\pi^-\pi^+\pi^0\nu_\tau$ (ex. K^0, ω, η)	0.0394 ± 0.0142	1.0000
$\pi^-2\pi^0\omega\nu_\tau$ (ex. K^0)	0.0071 ± 0.0016	1.0000
$2\pi^-\pi^+3\pi^0\nu_\tau$ (ex. K^0, η, ω, f_1)	0.0014 ± 0.0027	1.0000
$3\pi^-2\pi^+\nu_\tau$ (ex. K^0, ω, f_1)	0.0769 ± 0.0030	1.0000
$K^-2\pi^-2\pi^+\nu_\tau$ (ex. K^0)	0.0001 ± 0.0001	1.0000
$2\pi^-\pi^+\omega\nu_\tau$ (ex. K^0)	0.0084 ± 0.0006	1.0000
$3\pi^-2\pi^+\pi^0\nu_\tau$ (ex.K^0, η, ω, f_1)	0.0038 ± 0.0009	1.0000
$K^-2\pi^-2\pi^+\pi^0\nu_\tau$ (ex. K^0)	0.0001 ± 0.0001	1.0000
$\pi^- f_1\nu_\tau$ ($f_1 \to 2\pi^-2\pi^+$)	0.0052 ± 0.0004	1.0000
$\pi^-2\pi^0\eta\nu_\tau$	0.0194 ± 0.0038	1.0000

Table 6.1: τ branching fractions.

6.2 Derivation of New Kinematics

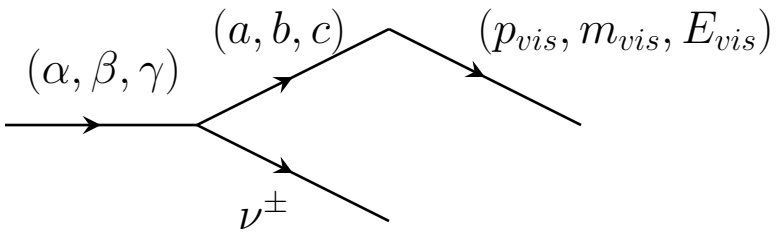

The τ direction is given by (α, β, γ) and the direction from the secondary vertex to where the visible products are created is (a, b, c). The visible products have information given by $(p_{vis}, m_{vis}, E_{vis})$, where p_{vis}, m_{vis}, E_{vis} are the momentum, mass, and energy of the visible products, respectively. We seek to find the τ momentum. We define the momentum of the tau as p_τ, the mass of the tau as m^τ, and the energy of the tau as E_τ. Lastly, we let p_ν, m_ν, E_ν be the momentum, mass, and energy of the neutrino, respectively.

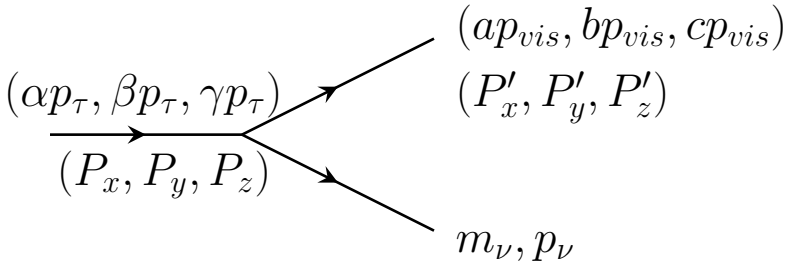

By conservation of momentum we have that

$$p_\nu = (P_x - P'_x, P_y - P'_y, P_z - P'_z)$$
$$E_\nu = E_\tau - E_{vis}.$$

Using $E_\nu^2 = P_\nu^2 + m_\nu^2$ and $E_\tau^2 = P_x^2 + P_y^2 + P_z^2 + m_\tau^2$ we find

$$
\begin{aligned}
(E_\tau - E_\nu)^2 &= (P_x - P'_x)^2 + (P_y - P'_y)^2 + (P_z - P'_z)^2 + m_\nu^2 \\
E_\tau^2 - 2E_\tau E_{vis} + E_{vis}^2 &= (P_x - P'_x)^2 + (P_y - P'_y)^2 + (P_z - P'_z)^2 + m_\nu^2 \\
m_\tau^2 - 2E_\tau E_{vis} + m_{vis}^2 &= -2(P_x P'_x + P_y P'_y + P_z P'_z) + \cancel{m_\nu^2} \\
m_\tau^2 - 2E_\tau E_{vis} + m_{vis}^2 &= -2p_\tau p_{vis}(\alpha a + \beta b + \gamma c)
\end{aligned}
$$

Rewriting the previous equation we have

$$(m_\tau^2 + m_{vis}^2) + 2p_\tau p_{vis}(\alpha a + \beta b + \gamma c) = 2E_\tau E_{vis}.$$

We now define

$$M = \frac{m_\tau^2 + m_{vis}^2}{2E_{vis}}, \quad C = \frac{p_{vis}(\alpha a + \beta b + \gamma c)}{E_{vis}}.$$

Thus, we are able to write our equation as

$$M + p_\tau C = E_\tau.$$

Squaring both sides we obtain

$$E_\tau^2 = M^2 + 2MCp_\tau + p_\tau^2 C^2.$$

Putting this into a convenient form we have

$$(1 - C^2)p_\tau^2 - 2MCp_\tau + (m_\tau^2 - M^2) = 0.$$

Using the quadratic formula we obtain

$$|p_\tau| = \frac{MC \pm \sqrt{M^2C^2 - (1 - C^2)(m_\tau^2 - M^2)}}{(1 - C^2)}.$$

This gives a new way for obtaining the momentum of the τ. Given a Z decay, we can use this to find the momentum for both τ^+ and τ^-.

6.3 Particle Identification Numbers

QUARKS	
d	1
u	2
s	3
c	4
b	5
t	6
b'	7
t'	8

LEPTONS	
e^-	11
ν_e	12
μ^-	13
ν_μ	14
τ^-	15
ν_τ	16
τ'^-	17
$\nu_{\tau'^-}$	18

GAUGE AND HIGGS BOSONS	
g	(9) 21
γ	22
Z^0	23
W^+	24
h^0/H_1^0	25
Z'/Z_2^0	32
Z''/Z_3^0	33
W'/W_2^+	34
H^0/H_2^0	35
A^0/H_3^0	36
H^+	37

LIGHT BARYONS	
p	2212
n	2112
Δ^{++}	2224
Δ^+	2214
Δ^0	2114
Δ^-	1114

LIGHT $I = 1$ MESONS	
π^0	(9) 21
π^+	22
$a_0(980)^0$	23
$a_0(980)^+$	24
$\pi(1300)^0$	100111
$\pi(1300)^+$	100211
$a_0(1450)^0$	10111
$a_0(1450)^+$	10211
$\pi(1800)^0$	9010111
$\pi(1800)^+$	9010211
$\rho(770)^0$	113
$\rho(770)^+$	213
$b_1(1235)^0$	10113
$b_1(1235)^+$	10213
$a_1(1260)^0$	20113
$a_1(1260)^+$	20213
$\pi_1(1400)^0$	9000113
$\pi_1(1400)^+$	9000213
$\rho(1450)^0$	100113
$\rho(1450)^+$	100213
$\pi_1(1600)^0$	9010113
$\pi_1(1600)^+$	9010213
$a_1(1640)^0$	9020113*
$a_1(1640)^+$	9020213*
$\rho(1700)^0$	30113
$\rho(1700)^+$	30213
$\rho(1900)^0$	9030113*
$\rho(1900)^+$	9030213*
$\rho(2150)^0$	9040113*
$\rho(2150)^+$	9040213*
$a_2(1320)^0$	115
$a_2(1320)^+$	215
$\pi_2(1670)^0$	10115
$\pi_2(1670)^+$	10215
$a_2(1700)^0$	9000115*
$a_2(1700)^+$	9000215*
$\pi_2(2100)^0$	9010115*
$\pi_2(2100)^+$	9010215*
$\rho_3(1690)^0$	117
$\rho_3(1690)^+$	217
$\rho_3(1990)^0$	9000117
$\rho_3(1990)^+$	9000217
$\rho_3(2250)^0$	9010117
$\rho_3(2250)^+$	9010217
$a_4(2040)^0$	119
$a_4(2040)^+$	219

6.4 MC Samples

Process	cross-section [pb]	Official CMS Datasets (MINIAODSIM)
$Z \to ll$ HT binned LO	5765.37995 (NNLO)	*/DYJetsToLL_M-50_TuneCUETP8M1_13TeV*
	226 (NNLO)	*/DYJetsToLL_M-100to200_TuneCUETP8M1_13TeV*
	7.67 (NNLO)	*/DYJetsToLL_M-200to400_TuneCUETP8M1_13TeV*
	0.423 (NNLO)	*/DYJetsToLL_M-400to500_TuneCUETP8M1_13TeV*
	0.24 (NNLO)	*/DYJetsToLL_M-500to700_TuneCUETP8M1_13TeV*
	0.035 (NNLO)	*/DYJetsToLL_M-700to800_TuneCUETP8M1_13TeV*
	0.030 (NNLO)	*/DYJetsToLL_M-800to1000_TuneCUETP8M1_13TeV*
	0.016 (NNLO)	*/DYJetsToLL_M-1000to1500_TuneCUETP8M1_13TeV*
	0.002 (NNLO)	*/DYJetsToLL_M-1500to2000_TuneCUETP8M1_13TeV*
	0.00054 (NNLO)	*/DYJetsToLL_M-2000to3000_TuneCUETP8M1_13TeV*
W+jets HT binned LO	61526.5082 (NNLO)	*/WJetsToLNu_HT-0To70_ext2-v1_RunIISummer16MiniAODv2-madgraphMLM-pythia8*
	61526.5082 (NNLO)	*/WJetsToLNu_HT-0To70_v1_RunIISummer16MiniAODv2-madgraphMLM-pythia8*
	1600.97582 (NNLO)	*/WJetsToLNu_HT-70To100_RunIISummer16MiniAODv2-madgraphMLM-pythia8*
	1632.5341 (NNLO)	*/WJetsToLNu_HT-100To200_ext1-v1_RunIISummer16MiniAODv2-madgraphMLM-pythia8*
	1632.5341 (NNLO)	*/WJetsToLNu_HT-100To200_ext2-v1_RunIISummer16MiniAODv2-madgraphMLM-pythia8*
	1632.5341 (NNLO)	*/WJetsToLNu_HT-100To200_v1_RunIISummer16MiniAODv2-madgraphMLM-pythia8*
	436.59666 (NNLO)	*/WJetsToLNu_HT-200To400_ext1-v1_RunIISummer16MiniAODv2-madgraphMLM-pythia8*
	436.59666 (NNLO)	*/WJetsToLNu_HT-200To400_ext2-v1_RunIISummer16MiniAODv2-madgraphMLM-pythia8*
	436.59666 (NNLO)	*/WJetsToLNu_HT-200To400_v1_RunIISummer16MiniAODv2-madgraphMLM-pythia8*
	59.3659798 (NNLO)	*/WJetsToLNu_HT-400To600_ext1-v1_RunIISummer16MiniAODv2-madgraphMLM-pythia8*
	59.3659798 (NNLO)	*/WJetsToLNu_HT-400To600_v1_RunIISummer16MiniAODv2-madgraphMLM-pythia8*
	14.626049 (NNLO)	*/WJetsToLNu_HT-600To800_ext1-v1_RunIISummer16MiniAODv2-madgraphMLM-pythia8*
	14.626049 (NNLO)	*/WJetsToLNu_HT-600To800_v1_RunIISummer16MiniAODv2-madgraphMLM-pythia8*
	6.67700378 (NNLO)	*/WJetsToLNu_HT-800To1200_ext1-v1_RunIISummer16MiniAODv2-madgraphMLM-pythia8*
	6.67700378 (NNLO)	*/WJetsToLNu_HT-800To1200_v1_RunIISummer16MiniAODv2-madgraphMLM-pythia8*
	1.6131136 (NNLO)	*/WJetsToLNu_HT-1200To2500_ext1-v1_RunIISummer16MiniAODv2-madgraphMLM-pythia8*
	1.6131136 (NNLO)	*/WJetsToLNu_HT-1200To2500_v1_RunIISummer16MiniAODv2-madgraphMLM-pythia8*
	0.03903516 (NNLO)	*/WJetsToLNu_HT-2500ToInf_ext1-v1_RunIISummer16MiniAODv2-madgraphMLM-pythia8*
	0.03903516 (NNLO)	*/WJetsToLNu_HT-2500ToInf_v1_RunIISummer16MiniAODv2-madgraphMLM-pythia8*
Top quark	831.76 (NNLO)	*/TT_TuneCUETP8M2T4_13TeV_RunIISummer16MiniAODv2_PUMoriond17_80X_mcRun2*
	80.95 (LO)	*/ST_t-channel_antitop_4f_inclusiveDecays_13TeV_RunIISummer16MiniAODv2_PUMoriond17_80X_mcRun2-powhegV2-madspin-pythia8_TuneCUETP8M1*
	136.02 (LO)	*/ST_t-channel_top_4f_inclusiveDecays_13TeV_RunIISummer16MiniAODv2_PUMoriond17_80X_mcRun2-powhegV2-madspin-pythia8_TuneCUETP8M1*
	35.6 (LO)	*/ST_tW_antitop_5f_inclusiveDecays_13TeV_RunIISummer16MiniAODv2_PUMoriond17_80X_mcRun2-powheg-pythia8_TuneCUETP8M1*
	35.6 (LO)	*/ST_tW_top_5f_inclusiveDecays_13TeV_RunIISummer16MiniAODv2_PUMoriond17_80X_mcRun2-powheg-pythia8_TuneCUETP8M1*
WW	63.21 (LO)	*/WW_TuneCUETP8M1_13TeV_RunIISummer16MiniAODv2_PUMoriond17_80X_mcRun2-pythia8*
WZ	22.82 (LO)	*/WZ_TuneCUETP8M1_13TeV_RunIISummer16MiniAODv2_PUMoriond17_80X_mcRun2-pythia8*
ZZ	10.32 (LO)	*/ZZ_TuneCUETP8M1_13TeV_RunIISummer16MiniAODv2_PUMoriond17_80X_mcRun2-pythia8*